RSC Sustainability

ROYAL SOCIETY OF CHEMISTRY

PAPER

View Article Online
View Journal | View Issue

Cite this: *RSC Sustainability*, 2025, **3**, 1434

Soybean oil-derived, non-isocyanate polyurethane–TiO_2 nanocomposites with enhanced thermal, mechanical, hydrophobic and antimicrobial properties†

Jaydip D. Bhaliya,[a] S. N. Raju Kutcherlapati,*[ac] Nikhil Dhore,[a] Neelambaram Punugupati,[ac] Kavya Lekha Sunkara,[b] Sunil Misra[bc] and Shivam Shailesh Kumar Joshi[ac]

This study explores the development of non-isocyanate polyurethane (NIPU) composites incorporating bio-based soybean oil and TiO_2 nanoparticles (TNPs) with enhanced functional properties. Epoxidized soybean oil (ESBO) was converted to 5-membered cyclic carbonated soybean oil (CSBO) through CO_2 insertion under high temperature and pressure. TNPs (0%, 0.25%, 0.5%, and 1%) were incorporated into CSBO and cured with ethylenediamine (EDA). ATR-FTIR analysis confirmed the formation of urethane linkages in the NIPU films. The impact of TNPs on the physiochemical properties of the NIPU films was evaluated, including mechanical, thermal, surface wetting, and antimicrobial performance. Thermogravimetric analysis (TGA) indicated that TNPs did not significantly alter the degradation temperature of the NIPU films, whereas Differential Scanning Calorimetry (DSC) revealed that the glass transition temperature (T_g) of the NIPU films increased from 24 °C to 27 °C with TNP loading. Mechanical properties showed increased tensile strength with higher TNP content, while elongation at break decreased. Surface wettability measurements demonstrated that all composite films exhibited hydrophobic behavior, with contact angles ranging from 97° to 105°, higher than those of the bare NIPU films. Antimicrobial testing against *Escherichia coli* and *Staphylococcus aureus* demonstrated that TNP-loaded NIPU films exhibited significant antimicrobial activity against *E. coli* and antifouling properties against *S. aureus*. These bio-based NIPU composites offer a sustainable alternative to petroleum-based polyurethanes, with potential applications in eco-friendly adhesives, antimicrobial coatings, and protective surfaces, thereby contributing to greener solutions in materials science.

Received 20th September 2024
Accepted 14th January 2025

DOI: 10.1039/d4su00587b

rsc.li/rscsus

Sustainability spotlight

The global shift toward sustainable materials has intensified the need for eco-friendly alternatives to traditional, petroleum-based polyurethanes, which often release harmful chemicals. Our research addresses this by developing non-isocyanate polyurethane (NIPU) composites derived from renewable soybean oil, enhanced with TiO_2 nanoparticles. These materials not only reduce dependence on fossil fuels but also eliminate toxic isocyanates, offering a safer, non-toxic solution for applications in coatings and adhesives. The TiO_2-incorporated NIPU films exhibit superior antimicrobial properties, along with enhanced thermal stability, mechanical strength, and hydrophobicity, making them suitable for high-performance, environmentally responsible applications. This work aligns with the UN's Sustainable Development Goals by reducing hazardous chemicals (SDG 3), promoting the use of renewable resources (SDG 12), and advancing sustainable industrial processes (SDG 9), contributing to a greener future.

1. Introduction

In recent years, renewable and plant-based polymeric materials have attracted significant attention due to growing economic and environmental concerns. Plant oils, in particular, have been extensively researched as starting materials for bio-based polymers, given their accessibility, availability, biodegradability, and green origins.[1,2] Plant oils have been successfully polymerized using various methods, including cationic,[3,4] metathesis,[2,5] free-radical,[6,7] and addition polymerization,[8,9] resulting

[a]*Polymers and Functional Materials Department, CSIR-Indian Institute of Chemical Technology, Uppal Road, Tarnaka, Hyderabad, Telangana, 500007, India. E-mail: ksnraju@iict.res.in*

[b]*Department of Applied Biology, CSIR-Indian Institute of Chemical Technology, Uppal Road, Tarnaka, Hyderabad, Telangana, 500007, India*

[c]*Academy of Scientific and Innovative Research (AcSIR), Ghaziabad, 201002, India*

† Electronic supplementary information (ESI) available. See DOI: https://doi.org/10.1039/d4su00587b

in a broad range of thermomechanical properties that span from flexible rubbers to rigid plastics.[10] Metathesis is an effective method for synthesizing bio-based polymers, such as diols and polyols, for polyurethane (PU) production by utilizing essential oils, fatty alcohols, and terpenes to replace petroleum-based sources.[11,12] Xia *et al.* reported the creation of soft to tough copolymers through cationic copolymerization using linseed oil and dicyclopentadiene.[3,4] Sheet molding compounds (SMCs) can also be made by replacing petroleum-derived materials with soybean oil and divalent metallic oxides *via* free radical polymerization.[6] Demchuk *et al.* explored the free radical polymerization of vinyl monomers from plant oil triglycerides.[7] Wang, Tang, and colleagues have enhanced bio-based polymers by combining novel chemical structures with unidirectional processing to produce ultra-strong polyamide elastomers from castor oil through thiol-ene addition polymerization.[9] Such versatility highlights their potential to replace petroleum-based polymers across various industries.

Polyurethanes (PUs) rank among the top six most manufactured polymers globally due to their versatility and diverse properties. The global PU market was valued at $72.82 billion in 2021 and is projected to grow at a compound annual growth rate (CAGR) of 4.3% from 2022 to 2030.[13] PUs are integral to a broad range of industries, including automotive, construction, medical devices, adhesives, coatings, and packaging.[14] However, conventional PU production relies heavily on isocyanates derived from toxic precursors such as phosgene, raising serious concerns regarding environmental safety and human health risks, including skin irritation and chronic respiratory diseases.[15] Additionally, the production and application of these materials often lead to the emission of volatile organic compounds (VOCs) and hazardous air pollutants (HAPs), which further contribute to environmental degradation.[16] In response, a global movement toward more environmentally friendly polyurethane alternatives has emerged, driven by stricter regulations and consumer demand for safer, low-VOC, bio-based materials.

Non-isocyanate polyurethanes (NIPUs) have gained prominence as a sustainable alternative, offering an eco-friendly route to polyurethane synthesis without the use of harmful isocyanates. NIPUs are typically formed by the reaction of cyclic carbonates with amines, producing urethane linkages more safely.[17] Various renewable resources, including vegetable oils, have been explored for NIPU synthesis due to their abundant availability and potential for functionalization.[17,18] Castor oil, with inherent hydroxyl groups, is often used directly in polyurethane formulations, while other oils like soybean oil require chemical modification, such as epoxidation and subsequent CO_2 insertion to form cyclic carbonates.[19–31]

Soybean oil, in particular, is an attractive candidate for bio-based NIPUs due to its global availability and favorable triglyceride structure, which consists of three fatty acids connected by a glycerol backbone.[14,15] Modifying these triglycerides to produce CSBO allows for the creation of NIPU through polyaddition with diamines. In a notable example, Javni *et al.* successfully synthesized NIPUs by reacting CSBO with diamines *via* a non-isocyanate approach.[32] Following similar principles, this study employs CSBO, derived from epoxidized soybean oil (ESBO) through CO_2 insertion, and cross-links it with ethylenediamine (EDA) to form NIPU films. ESBO has already found applications in the PVC industry as a plasticizer and stabilizer due to its cost-effectiveness and beneficial properties such as low viscosity, odorlessness, and high functionality.[15,33–35]

To further enhance the properties of the resulting NIPUs, some of the metal nanoparticles, such as ZnO, TiO_2, Cu, CuO, Ag, and Au, were incorporated into the polymer matrix.[36] Gholami *et al.* reported a similar study of soybean oil-derived NIPU containing azetidinium groups for antimicrobial applications and *in situ* formed nano-silver for antimicrobial wound dressing applications.[37,38] In comparison, TiO_2 nanoparticles are biocompatible, non-toxic, and environmentally safe, unlike nanosilver, which raises concerns due to potential cytotoxicity, environmental accumulation, and antimicrobial resistance. Additionally, TiO_2 nanoparticles provide long-term antimicrobial activity and multifunctionality, including enhanced mechanical strength, thermal stability, and hydrophobicity, without the leaching issues associated with nanosilver. Compared to azetidine-functionalized polyurethanes, which involve complex chemical modifications and limited antimicrobial scope, our approach is more straightforward and scalable while ensuring broad-spectrum antimicrobial efficacy through photocatalytic mechanisms. Furthermore, our synthesis method avoids hazardous reagents like isocyanates and phosgene, aligning with sustainable and eco-friendly material development goals. These distinctions highlight the novelty of our work, offering a safer, more sustainable, and multifunctional alternative for antimicrobial polyurethane films. TiO_2 is well known for its excellent mechanical reinforcement, thermal stability, and antimicrobial properties.[36] The addition of TiO_2 nanoparticles has been shown to significantly improve the surface hydrophobicity, mechanical strength, and antimicrobial efficacy of polymeric films. Such properties are critical for various applications, including antimicrobial coatings, medical devices, and protective surface treatments.[10] Despite these advantages, soybean oil-based NIPU composites containing TNPs have not been extensively studied, presenting an opportunity to explore novel material properties and applications.

In this study, NIPU films were synthesized by curing carbonated soybean oil (CSBO) with ethylenediamine (EDA). The influence of varying concentrations of titanium dioxide nanoparticles (TNPs) on the films was examined, focusing on their antimicrobial activity, surface wettability, mechanical properties, and thermal performance. This research underscores the promise of sustainable, bio-based NIPUs as a feasible replacement for traditional polyurethanes, supporting the expanding field of green chemistry and sustainable materials science.

2. Experimental section

2.1 Materials

Epoxidized soybean oil was obtained from Makwell Organic Private Limited, Mumbai, India. Titanium dioxide (TiO_2)

nanoparticles (TNPs) were purchased from Sigma-Aldrich Chemicals Pvt Ltd, and ethylene diamine was purchased from Spectrochem Pvt Ltd Mumbai, India. Dipropylene glycol monomethyl ether (mixture of isomers) extra pure 99% was purchased from Sisco Research Laboratories (SRL) Pvt. Ltd, and 3-hydroxy-2,2,4-trimethylpentyl isobutyrate (texanol) was purchased from TCI. Kosmos (stannous octoate) was purchased from Goldschmidt Gmbh, Essen, Germany. Tetrabutylammonium bromide (TBABr), hydrobromic acid (HBr, 46%), acetic acid, and hydrochloric acid (HCl) were obtained from Finar Chemicals Pvt. Ltd.

2.2 Methods

2.2.1 Synthesis of carbonated soybean oil (CSBO). Carbonated soybean oil was synthesized by coupling CO_2 with epoxidized soybean oil in a high-pressure reactor (Amar Equipment Pvt. Ltd, Mumbai, India, having a capacity of 1 L volume, vessel design with −1 to 100 bar pressure, and −10 to 250 °C temperature operating conditions) as shown in Scheme 1 as per the discussed synthesis process in our previous report.[14,33] In the reaction vessel, approximately 250 g of ESBO and tetrabutylammonium bromide (TBAB, 8.8 wt% of ESBO) were added. Then, the reaction mixture was heated to 120 °C with continuous stirring. CO_2 was passed into the reactor with a 20 bar pressure and maintained during the entire course of the reaction for the next 24 h. After the completion of the reaction, clear brownish viscous oil was collected at 60–70 °C (to afford free-flowing liquid oil, Fig. S1†). CO_2 insertion was also confirmed by FT-IR and ^{1}H NMR.[14,33] ESBO to CSBO conversion was reported in our previous report[33] and the same material was used for this study.

2.2.2 Preparation of NT-*X* nanocomposite films. Predetermined quantities of CSBO were combined with varying concentrations of TNPs to fabricate NIPU composite films. The preparation of NIPU composites was started by incorporating the necessary components into the CSBO, followed by 30 minutes of homogenization to ensure uniform dispersion. Initially, the CSBO was weighed precisely, and stannous octoate was introduced as a catalyst at ambient temperature. Subsequently, the formulation was supplemented with different TNP concentrations (NT-*X*, *X* = 0%, 0.25%, 0.5%, and 1%), resulting in NIPU, NT-0.25, NT-0.5, and NT-1 films, respectively (Table 1 and Scheme 2). These variations were intended to enhance the antimicrobial properties of the films. The mixture was then sonicated for 30 minutes, and a coalescing solvent mixture was incorporated to reduce the viscosity of the NT-*X* dispersions. Finally, an EDA curing agent, at 13 wt% relative to CSBO, was added and thoroughly combined. The films were cast into silicon molds and cured at 80 °C for 24 hours, followed by an additional 4 h of curing at 110 °C (Fig. S4†). The produced nanocomposite films were subjected to various characterization techniques to evaluate their physical, thermal, and antimicrobial properties.

2.2.3 Characterization. A PerkinElmer (Spectrum-1000, Waltham, MA, USA) spectrophotometer instrument was used for functional group identification of monomers and polymers by FT-IR (Fourier Transform Infra-Red) spectroscopy. The samples were smeared on KBr pallets and scanned from 4000 to 400 cm^{-1} with 8 scans on average at a resolution of 4 cm^{-1} and the IR spectra were recorded. Meanwhile, the FT-IR of the prepared films was conducted in Attenuated Total Reflection (ATR) mode in a scan range from 4000 to 400 cm^{-1} with a resolution of 4 cm^{-1} by performing 40 scans.

Nuclear Magnetic Resonance Spectroscopy (^{1}H NMR) spectra of ESBO and CSBO were recorded with the help of a BRUKER AVANCE-400 MHz spectrometer at ambient temperature in $CDCl_3$ solution. The mechanical properties of the film were

Table 1 Formulation for the cast NT-*X* composite films

Sample	CSBO (g)	Catalyst (g)	EDA (g)	TNPs (g)
NIPU	5	0.1	0.650	—
NT-0.25	5	0.1	0.650	0.015
NT-0.5	5	0.1	0.650	0.03
NT-1	5	0.1	0.650	0.06

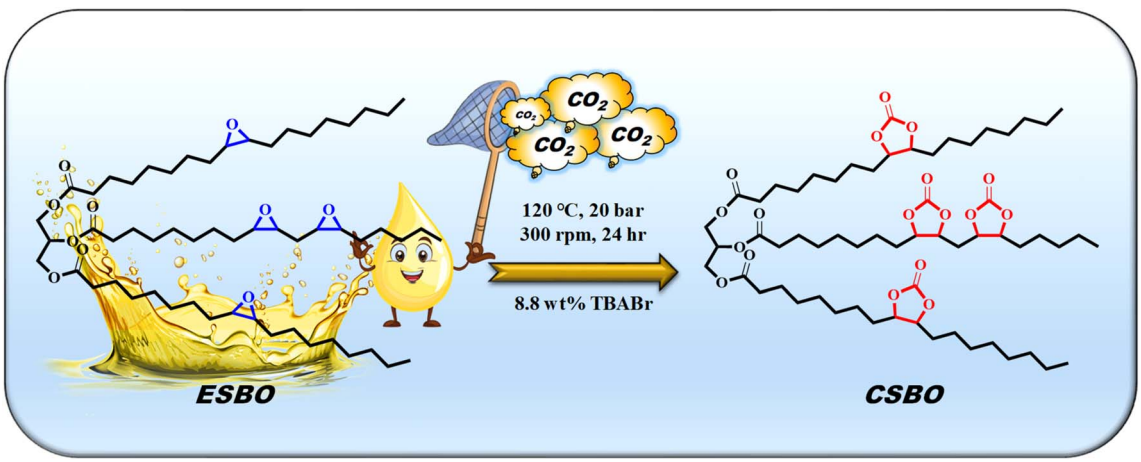

Scheme 1 Synthesis of CSBO from ESBO.

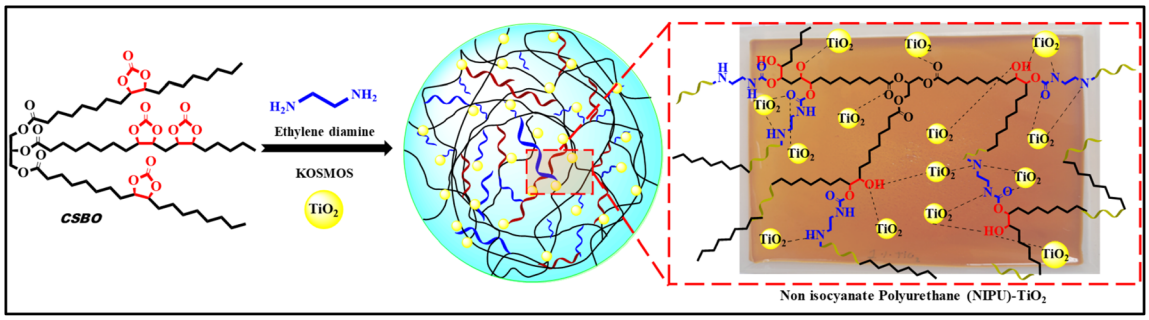

Scheme 2 Synthesis of NT-*X* films from CSBO.

tested by a tensile test using a Universal Testing Machine (UTM) (Dak System Inc.; model no. T-72502). The UTM was equipped with a 100 kg load cell and 50 mm gauge length with a cross-head speed of 10 mm min^{-1} as per ASTM D882. The specimen had the following dimensions: 0.5 mm thickness and a length and width of nearly about 110 mm and 10 mm, respectively, and two samples of each specimen were tested to obtain an average value of each group.

A DSC Q100 EXFO Series 2000 model from TA Instruments was used to record the DSC curve of the prepared NT-*X* composite films. The glass transition temperature of the films was determined at a heating rate of 10 °C min^{-1} with about ~8–10 mg of each sample under a nitrogen atmosphere in the −70 °C to 150 °C temperature range. The heating cycle for each sample began with the first cycle, where the temperature was increased from −70 °C to 150 °C. In the second cycle, the sample was cooled down to −70 °C, followed by a third cycle in which it was reheated from −70 °C to 150 °C.

A Dynamic Mechanical Analyzer (DMA Q800, TA Instruments) was used to conduct DMTA studies on NIPU films that were properly cut. Under nitrogen, the samples were evaluated at a fixed frequency of 1 Hz and a heating rate of 10 °C min^{-1} to determine the rheological characteristics, such as storage modulus and loss or damping factor (tan δ). The tan δ curves provided the glass transition temperature of the NIPU films.

The Water Contact Angle (WCA) of the NIPU was evaluated as a measure of hydrophilicity using a G10 Goniometer (KRÜSS instrument, Hamburg, Germany) by applying the captive bubble technique through a stalkless drop at ambient conditions. The WCA, as a measure of hydrophobicity, was evaluated after 10 days of sample preparation on a glass side coating and a water droplet was poured on the coated surface with a micro-syringe fitted in instruments to obtain the average value of 5–6 replicates performed on each sample.

The SEM analysis of the TNPs incorporated into NIPU films was carried out using a Hitachi-S520 (Oxford link ISIS SEM model), Japan, and a Zeiss Merlin Compact Model for the surface smoothness and particle dispersion into a film. The elemental mapping of the film was studied through Energy-Dispersive Spectroscopy (EDS) combined with FE-SEM. The materials were dried in the air before use.

Thermogravimetric analysis (TGA) was performed using 5–10 mg of material on a TA Q500 (TA Instruments, New Castle, DE, USA) thermogravimetric analyzer under a N_2 environment from room temperature to 700 °C, with a heating rate of 10 °C min^{-1}.

The microbial growth inhibition studies of the NIPU were performed against a Gram-negative organism, *Escherichia coli* (MTCC 443), and a Gram-positive organism, *Staphylococcus aureus* (MTCC 96), using the conventional agar diffusion method.[10,39] The prepared nutrient-rich agar medium was poured into sterile Petri dishes under aseptic conditions. Once the medium in the plates had solidified, 0.5 mL of the test organism (106 CFU mL^{-1}) culture was evenly inoculated across the agar surface. To test microbial inhibition, each NIPU-based film was accurately cut into 1 cm × 1 cm specimens, washed thoroughly with distilled water, and carefully placed on the growth medium of the cultured microbial organisms. Finally, the microbial growth inhibition observed with the films was incubated for 24 hours at 37 °C. Streptomycin served as a positive control for comparison during the same period. The antimicrobial properties of the films were evaluated by measuring the clear zone of inhibition surrounding the films against each microbial strain.

Additionally, the antimicrobial activity of each NIPU film was further assessed by evaluating microbial growth inhibition at both 48 hours and 72 hours. Under these conditions, bacterial growth continued in the medium for the entire 72-hour duration. For determining antifouling properties, we analyzed the possible growth of microorganisms both on the surface and below the film. If growth occurred either on or below the surface of the film, it suggests a lack of antifouling activity. Conversely, if there was no growth observed on or below the surface of the film, it indicates antifouling activity.

3. Results and discussion

The conversion of ESBO to CSBO is crucial in the synthesis of non-isocyanate polyurethanes. While epoxies exhibit significant reactivity, curing epoxides on long alkyl chains, such as secondary epoxies, presents challenges due to their lower reactivity, frequently resulting in incomplete curing and suboptimal polymer network formation.[40–43] In contrast, the cyclic carbonates (in our case, CSBO) react effectively with amines, enabling the formation of urethane linkages without the need for toxic isocyanates. This transformation not only

addresses the limitations of secondary epoxies but also facilitates the development of sustainable, bio-based polyurethanes with enhanced environmental and functional performance.[44–46] The structural characterization of the ESBO and CSBO using epoxy values, FT-IR, ^{1}H NMR, and ^{13}C NMR was given in our earlier report[33] and is also presented in Fig. S2 and S3† for FT-IR and ^{1}H-NMR, respectively.

After confirming the formation of CSBO, EDA was employed as the curing agent for CSBO to make the NIPU network. The choice of EDA as the curing agent for CSBO is crucial due to the need for enhanced crosslinking density in NIPUs.[33,47] Soybean oil-based triglycerides, with their longer molecular chains and higher molecular weight, often result in lower crosslinking density and, consequently, reduced mechanical properties when cured with conventional amines.[32,48] EDA, with its small molecular structure and high reactivity, improves the crosslinking of CSBO, leading to stronger films with enhanced tensile strength. This is particularly important when working with bio-based materials, which typically exhibit lower reactivity and weaker mechanical properties compared to petroleum-based alternatives. By employing EDA, a higher degree of crosslinking is achieved, ensuring that the final films or coatings possess better mechanical integrity.[42,47] Furthermore, the incorporation of TNPs further enhances the NIPU's mechanical, hydrophobic, and antimicrobial properties, making it suitable for advanced applications in sustainable coatings and adhesives.

The physicochemical properties of the NIPU and NT-*X* films were investigated through extensive thermal, mechanical, spectroscopic, microscopic, and antimicrobial analyses and were discussed in the following section.

3.1 Fourier transform infrared spectroscopy of NT-*X* composites

The FTIR spectra of the NIPU exhibit peaks indicative of the formation of urethane linkages, as shown in Fig. 1. Specifically, peaks at 3303–3342 cm^{-1} and 1528 cm^{-1} correspond to the N–H stretching and bending of the urethane bond, respectively. Similarly, the C=O and C–N stretching of the urethane bond are responsible for peaks at 1699 and 1255 cm^{-1}, respectively. These findings confirm that the ring-opening of cyclic carbonate with amines leads to the synthesis of urethane bonds in the NIPU. Furthermore, the small carbonyl peak at 1809 cm^{-1} corresponds to the residual cyclic carbonate in NT-*X* composites.[33] The peaks of the coupling between NIPU and TiO_2 NPs in NT-*X* composites are located at 1255 cm^{-1} and 773 cm^{-1}, which are not distinguishable in FTIR spectra. Because NIPU has absorption peaks in these locations and the absorption level for C–O–Ti coordination is almost negligible compared to that of the NIPU peaks, there is not an additional peak between NIPU and NT-*X*.[49] A similar kind of response was reported by Kianpour *et al.*[49] for *in situ* synthesized TiO_2-polyurethane nanocomposites.

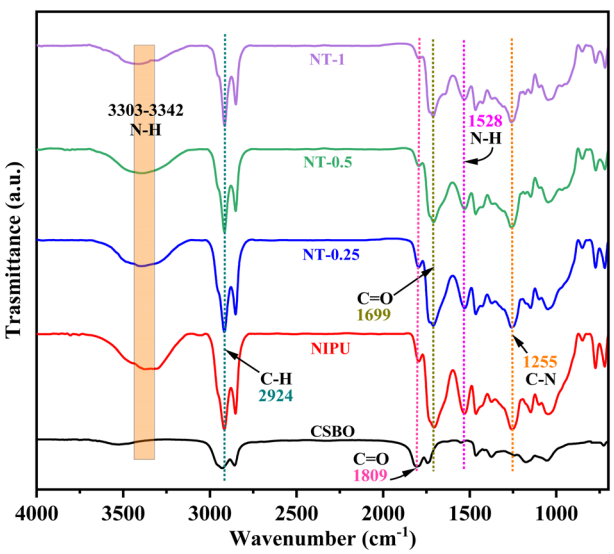

Fig. 1 ATR-FTIR spectra of NT-*X* composites.

3.2 Thermal analysis of NT-*X* composites

TGA was conducted on the NT-*X* composite films to evaluate their thermal stability and degradation behavior as a function of temperature, as depicted in Fig. 2. In the initial stage, from 50 to 230 °C, mass loss was attributed to the evaporation of physisorbed water and residual solvent molecules, as indicated by the $T_{d5\%}$ values. At this stage, no significant changes were observed in the NT-*X* films. The second degradation phase, occurring between 230 °C and 270 °C, is associated with the dissociation of urethane linkages within the NIPU matrix as seen in the DTG curve. The major weight loss observed between 270 °C and 450 °C is likely due to the decomposition of the long alkyl chains from the soybean oil component of the polymer as observed at a large peak in the DTG curve. Additionally, the final degradation stage, from 450 °C to 520 °C, is attributed to the breakdown of C–C and C–O bonds, leading to the thermal decomposition of the polymeric backbone. This is a three-stage degradation that occurs in NT-*X* composites as seen in the DTG curve in Fig. 2(b). Furthermore, the degradation temperatures corresponding to 5%, 10%, 50%, and 95% weight loss for the NIPU films with varying TNP concentrations are summarized in Table 2. A slight increase in $T_{d95\%}$ was noted, from 470 °C for the pure NIPU to 480 °C for NT-1, alongside a higher final ash content (at 700 °C) with increasing TNP concentration. This improvement in thermal stability can be attributed to the formation of tetrahedral O–Ti–O linkages within the polymer matrix through electrostatic interactions. Additionally, the hydrogen bonding between TNPs and the polymer backbone contributes to the enhanced thermal stability of the nanocomposite films.[50,51]

DSC curves for all NT-*X* films, obtained from the second heating scans, are presented in Fig. 3. The glass transition temperature (T_g) of the NIPU nanocomposite films was found to be near room temperature. Xu *et al.* reported on a self-healing glassy polyurethane with a T_g of 36.8 °C.[52] A slight increase in T_g was observed with the increasing concentration of TNPs, where the T_g values ranged from 24.25 °C for the pure NIPU film to 27.69 °C for the NT-1 film (1% TNPs). Specifically, the T_g

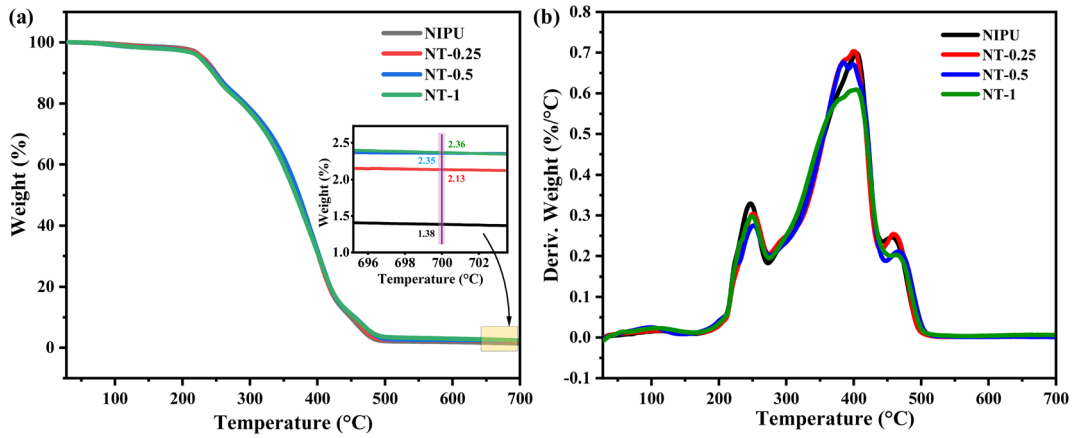

Fig. 2 (a) TGA and (b) DTG curves of 0 to 1% NT-*X* composite films.

Table 2 Thermal degradation data of NT-*X* composite films

	Degradation temperatures (°C)				
Sample	$T_{d5\%}$ (°C)	$T_{d10\%}$ (°C)	$T_{d50\%}$ (°C)	$T_{d95\%}$ (°C)	Residues at 700 °C (%)
NIPU	229.19	246.47	370.86	470.0	1.38
NT-0.25	229.98	229.71	372.12	473.45	2.13
NT-0.5	226.12	248.44	372.57	479.72	2.35
NT-1	225.87	245.94	367.81	480.42	2.36

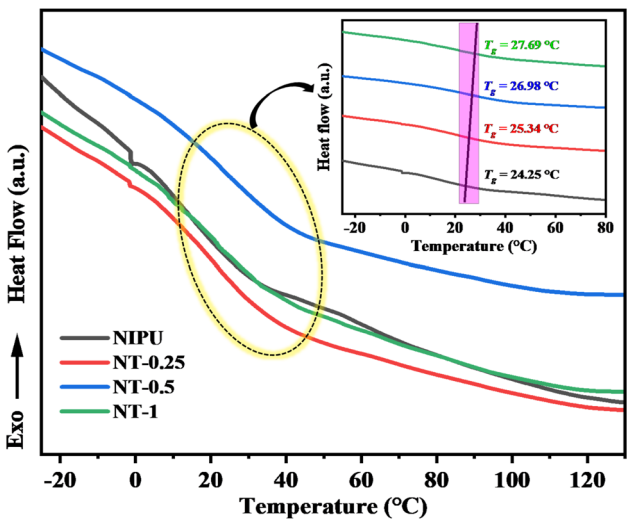

Fig. 3 DSC curves of NT-*X* films at different concentrations of TNPs.

values were 25.45 °C for NT-0.25, 26.98 °C for NT-0.5, and 27.69 °C for NT-1. The lowest T_g was observed in the pure NIPU film, which lacked fillers. As the concentration of TNPs increased, the T_g values progressively rose. This trend can be attributed to the surface hydroxyl groups present on the TNPs, which likely form hydrogen bonds with the –NH groups in the polymer backbone. These hydrogen bonds restrict the mobility of the polymer chains, leading to a reduction in the free volume within the crosslinked structure. This decrease in chain mobility, combined with the interaction between TNPs and the polymer matrix, results in the observed increase in T_g.[53,54]

3.3 Mechanical properties of NT-*X* composites

Dynamic mechanical thermal analysis was performed to measure the storage modulus (E') and tan δ of the NT-*X* films with varying TNP content, as shown in Fig. 4(a) and (b). The storage modulus increased with increasing TNP loading, due to the reinforcement effect of the nanoparticles, which hindered the mobility of the NIPU chains and enhanced interfacial stress transfer, leading to greater stiffness in the films. This indicates how TNPs strengthen the nanocomposite by improving the rigidity of the polymer matrix. As expected, the storage modulus decreased with increasing temperature, as the molecules within the polymer became more thermally active, leading to weaker intermolecular forces and reduced nanoparticle-matrix bonding.[55,56]

The rapid drop observed in E' of all films in the temperature range from −60 to 30 °C, corresponding to energy dissipation of the materials, is shown as the peak maximum in the tan δ curve.[57] The glass transition temperature of the NT-*X* films increased with TNP content, rising from 37.23 °C for NIPU to 45.8 °C for NT-1, consistent with the reinforcing effect of TNPs.[57–59] This increase in T_g is attributed to the strong interfacial interactions between the polymer matrix and the nanoparticles, which restrict the mobility of the polyurethane chains, further enhancing the mechanical properties of the films.[33,60,61] A similar kind of response was reported by Meera *et al.*[61] for silica NPs for a castor oil-based polyurethane nanocomposite and Chang *et al.*[62] for epoxy resin-silica nanocomposite materials.

The mechanical properties of the NT-*X* nanocomposite films were evaluated using a UTM, with the results presented in Fig. 5. The stress–strain behavior of all NT-*X* films exhibited an elastic response. As summarized in Table 3, the tensile strength of the NT-*X* films increased with the loading of TNPs, showing higher tensile strength compared to the bare NIPU film. This improvement in tensile strength can be attributed to the

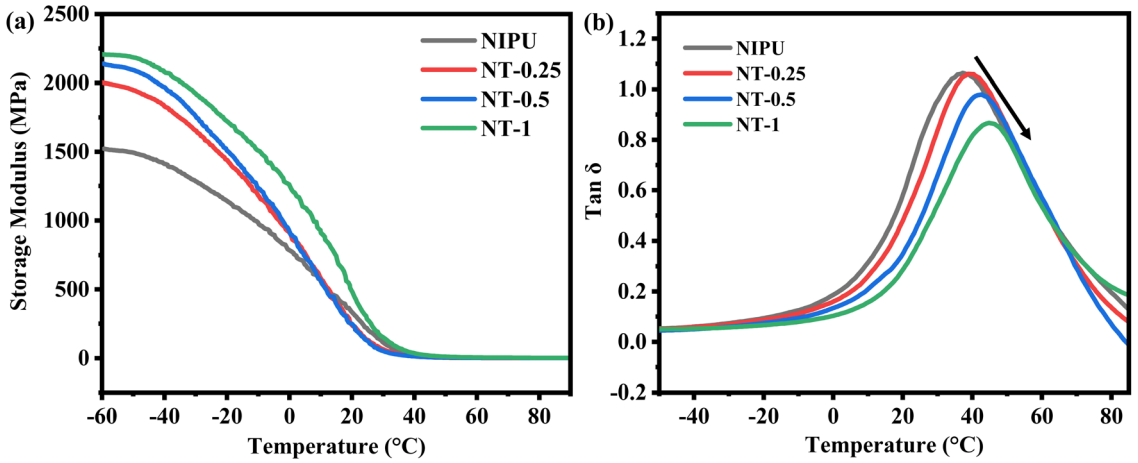

Fig. 4 DMTA curve of NT-*X* films: (a) storage modulus *vs.* temperature and (b) tan *δ* *vs.* temperature curves.

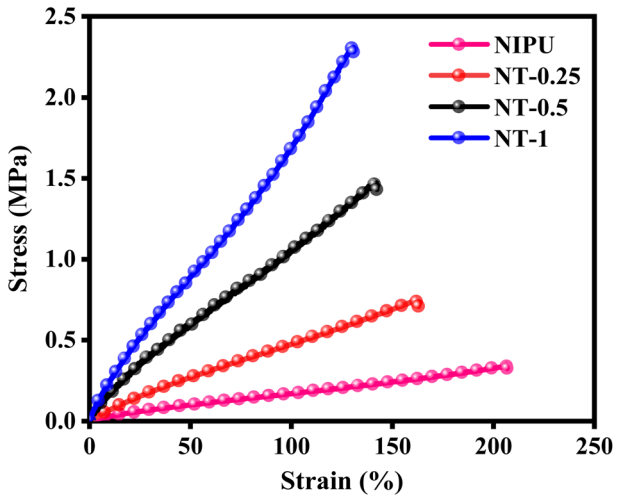

Fig. 5 Stress–strain curves of the NIPU, NT-0.25, NT-0.5, and NT-1 films.

reinforcing effect of the TNPs, which contribute to enhanced stress distribution within the NIPU matrix. However, as the TNP content increased, the elongation at break decreased, from 206.9% for NIPU to 130.9% for NT-1. This reduction in elongation is likely due to the decreased flexibility of the polymer matrix caused by the nanoparticles, which restrict the chain mobility.[53,63]

3.4 Surface morphology analysis of NT-*X* composites

The surface characteristics of NIPU and NT-*X* films were examined using field emission scanning electron microscopy (FE-SEM), both with and without TNPs, as presented in Fig. 6. The FE-SEM images demonstrate that the surface roughness of the films increased as the TNP content increased. The NIPU film (without TNPs) displayed a smooth surface, indicating minimal irregularities. Conversely, the NT-0.25, NT-5, and NT-1 films, containing TNPs, exhibited increased surface roughness, which may be due to enhanced cross-linking within the polymer matrix. As seen in Fig. 6(a) to (d), the formation of a microporous flake-like structure is evident due to the incorporation of TNPs.[33] As illustrated in Fig. 6, the TNPs were uniformly dispersed throughout the NIPU matrix.[33,64] This homogeneous distribution of nanoparticles contributed to the increase in surface roughness, which was further corroborated by the rise in the water contact angle, indicating a more hydrophobic surface.

Elemental mapping using energy-dispersive X-ray (EDX) spectroscopy was performed on the NIPU and NT-1 films to identify the distribution of key elements such as C, O, N, and Ti (Fig. S5† and 7). The results verified the uniform dispersion of TNPs throughout the NIPU polymer matrix, as seen in Fig. 7. This even distribution can be attributed to hydrogen bonding between the hydroxyl groups on the surface of the TNPs and the carbonyl or hydroxyl functional groups within the polymer. Additionally, physical forces such as van der Waals interactions

Table 3 Static mechanical properties of the NT-*X* composite films

Sample	Tensile strength (MPa)	Elongation at break (%)	Storage modulus (MPa) @−60 °C	T_g (°C)/tan *δ*
NIPU	0.33 ± 0.18	206.9 ± 0.1	1521	37.23
NT-0.25	0.71 ± 0.05	162.9 ± 13.7	2002	39.15
NT-0.5	1.43 ± 0.08	142.4 ± 17.3	2139	43.65
NT-1	2.28 ± 0.11	130.9 ± 17.1	2207	45.80

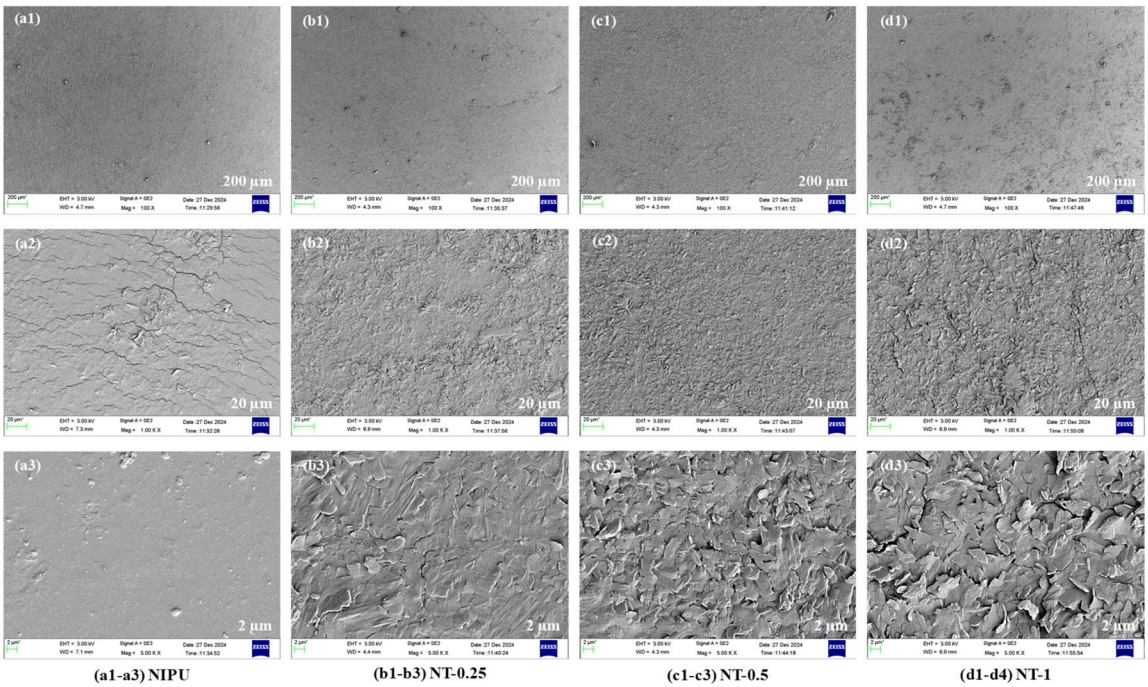

Fig. 6 FE-SEM images of the films: (a1)–(a3) NIPU, (b1)–(b3) NT-0.25, (c1)–(c3) NT-0.5, and (d1)–(d3) NT-1.

helped to prevent particle agglomeration, ensuring a stable and uniform dispersion of the nanoparticles within the composite films.[65,66]

3.5 Surface wettability of NT-*X* composites

The wettability of the NIPU and NT-*X* composite films was evaluated using water contact angle (WCA) measurements (Fig. 8), which revealed a clear trend toward increased hydrophobicity with the incorporation of TNPs. Hydrophilicity or hydrophobicity is determined by the WCA of a material: a WCA less than 90° indicates a hydrophilic surface, while a WCA greater than 90° denotes a hydrophobic surface. The NIPU films exhibited a WCA of 97°, suggesting a moderately hydrophobic nature due to the long alkyl chains in the soybean oil-derived

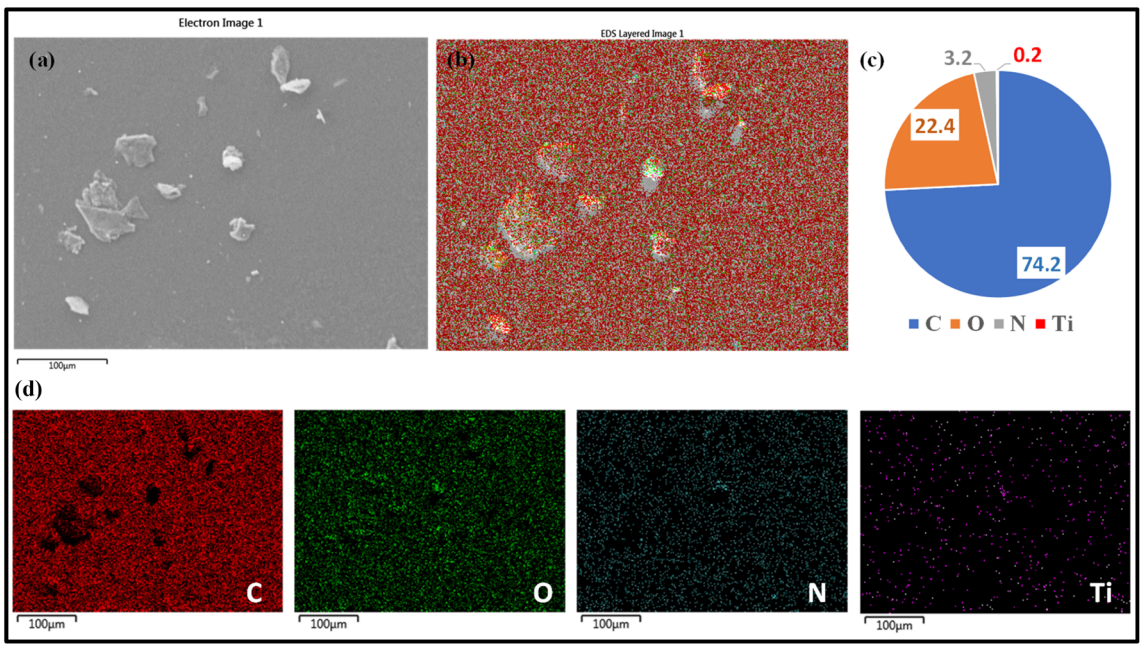

Fig. 7 (a) FE-SEM image, (b) EDS mapping, (c) EDX percentage distributions of elements, and (d) elemental mapping of C, O, N, and Ti for the NT-1 film.

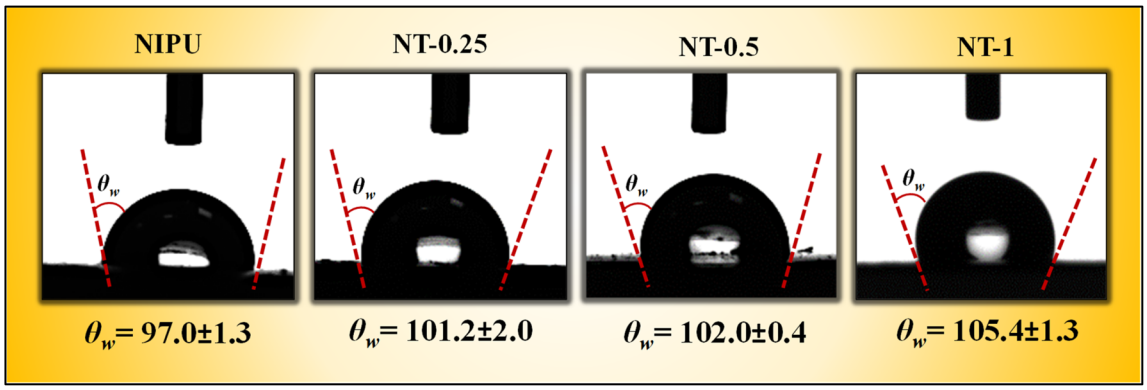

Fig. 8 Water contact angle (WCA) analysis of the prepared NIPU, NT-0.25, NT-0.5, and NT-1 composite films.

triglycerides, which naturally repel water.[33] However, when TNPs were incorporated, the WCA increased to 105° for the NT-*X* films, confirming a stronger hydrophobic behavior. The stability of the contact angle was measured over various time intervals for NT-*X* films, as shown in Table 4. The contact angle measurements remained relatively unchanged during the observed periods. This increase is attributed to the inherently hydrophobic nature of the Ti–O bonds within the TNPs, which reduces the surface's ability to interact with water molecules.[50,67]

The enhanced hydrophobicity is also linked to the increased surface roughness at the nanoscale caused by the presence of TNPs. As the nanoparticle loading increased, the crosslinking density within the polymer matrix also rose, as evidenced by the mechanical property data obtained through UTM and DMA. Increased crosslinking reduces the flexibility of the polymer chains and leads to greater surface irregularities at the nanoscale. This, in turn, results in greater air trapping at the surface, further decreasing the material's wettability and contributing to the overall hydrophobic behavior of the films. The combination of the inorganic TNPs within the organic NIPU matrix, coupled with the increased surface roughness, explains the enhanced water-repellent properties observed in the NT-*X* films.[50,68]

3.6 Antimicrobial activity of NT-*X* composites

The antimicrobial efficacy of NT-*X* composites with varying TNP loading (0–1%) was assessed against Gram-negative *Escherichia coli* and Gram-positive *Staphylococcus aureus* using the conventional agar diffusion method. The antimicrobial activity of the films was evaluated over 24 h, 48 h, and 72 h, with the results of the zone of inhibition (ZOI) studies presented in Fig. 9 and 10 and Table 5. It is known that any material with antimicrobial properties will not allow the growth of the bacteria, even when fully fledged in a bacterial medium.[39] In our case, *E. coli*, as depicted in Fig. 9, the NT-*X* films demonstrated a distinct zone of inhibition, indicating effective prevention of microbial growth around the composite films. The NIPU film without TNPs showed no ZOI, even after 72 h of incubation, suggesting negligible antimicrobial activity. In contrast, NT-*X* films with 0.25%, 0.5%, and 1% TNPs exhibited increasing inhibition zones of 1 mm, 2 mm, and 3 mm, respectively, after 72 h. The increasing ZOI with higher TNP loading suggests a dose-dependent antimicrobial effect. After 24 h, no bacterial growth was observed on any of the films. To comprehensively evaluate microbial resistance, the incubation was extended to 48 h and 72 h, revealing an increasing trend in the ZOI for NT-*X* films. Notably, no physical changes such as deformation or discoloration were observed in the films, even after 72 h of incubation, highlighting their structural stability and effective antimicrobial properties against *E. coli*.

Similarly, antimicrobial testing against *S. aureus*, shown in Fig. 10, revealed no significant ZOI for any of the films. However, the absence of microbial growth on the film surfaces, along with no observable changes in the film morphology (size, shape, or color), indicated antifouling activity. This suggests that while the NT-*X* films do not actively kill *S. aureus*, they inhibit microbial adhesion and proliferation on their surfaces.

The antimicrobial activity of the TNP-loaded NIPU films is likely attributable to the photocatalytic properties of TNPs. TNPs are known to generate reactive oxygen species (ROS), such as hydroxyl radicals and superoxide ions, upon exposure to UV or visible light. These ROS can damage microbial cell walls, disrupt cellular functions, and ultimately lead to cell death.[69,70] When embedded in the polymer matrix, TNPs act as active centers, continuously generating ROS under ambient light conditions, contributing to the antimicrobial efficacy of the NT-*X* films against both *E. coli* and *S. aureus*. In conclusion, the NT-*X* films demonstrated both antifouling and antimicrobial properties. The antifouling effect, particularly against *S. aureus*, was evident from the lack of microbial adhesion and growth on the film surface. For *E. coli*, the films exhibited robust antimicrobial activity by inhibiting bacterial growth around the films. The physicochemical interaction of bacterial cells with the film

Table 4 WCA of NT-*X* films with time

	WCA of NT-*X* films			
Time	NIPU	NT-0.25	NT-0.5	NT-1
Initially	97.9 ± 1.3	101.2 ± 2.0	102 ± 0.4	105.4 ± 1.3
After 7 days	97.0 ± 1.1	100.1 ± 0.6	101.1 ± 1	103.1 ± 0.9
After 16 days	98.5 ± 1.6	101.8 ± 0.9	102.1 ± 1.8	104.2 ± 2.1

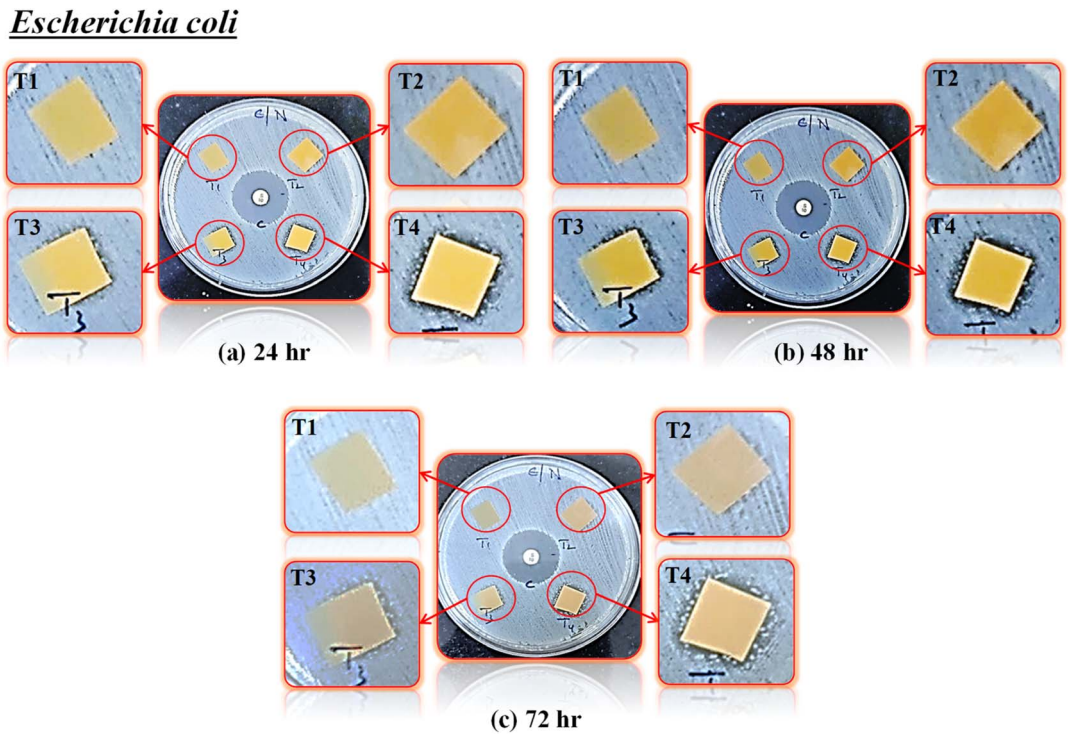

Fig. 9 Antimicrobial activity of the prepared NIPU (T1), NT-0.25 (T2), NT-0.5 (T3), and NT-1 (T4) films against *Escherichia coli* after (a) 24 h, (b) 48 h, and (c) 72 h.

surface is a key factor influencing microbial adhesion and proliferation.[71] As the WCA results from the previous section indicated, increasing TNP content enhances surface hydrophobicity, hindering microbial adhesion to the film. This dual-function behavior suggests that NT-*X* films not only possess potent antimicrobial activity but also effectively prevent

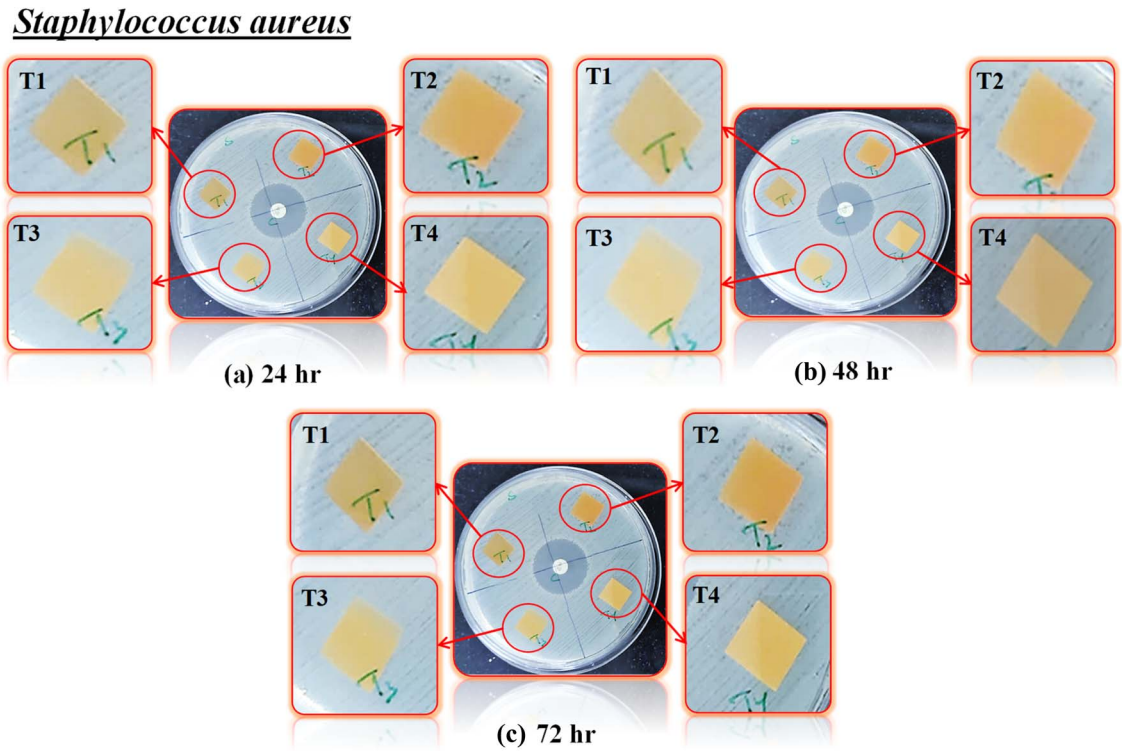

Fig. 10 Antimicrobial activity of the prepared NIPU (T1), NT-0.25 (T2), NT-0.5 (T3), and NT-1 (T4) films against *Staphylococcus aureus* after (a) 24 h, (b) 48 h, and (c) 72 h.

Table 5 Zone of inhibition against *E. coli* and *S. aureus* for NT-*X*

Sample	Zone of inhibition (mm) after 72 h	
	Gram-negative *Escherichia coli*	Gram-positive *Staphylococcus aureus*
NIPU	—	—
NT-0.25	1	—
NT-0.5	2	—
NT-1	3	—
Positive control (*Streptomycin*)	25	25

biofilm formation, contributing to their potential for advanced antimicrobial and antifouling applications.[72]

4. Conclusion

This study presents the development of non-isocyanate polyurethane (NIPU) nanocomposite films incorporating bio-based soybean oil and TNPs, using ethylenediamine (EDA) as the curing agent. FTIR analysis confirmed the successful synthesis of NIPU films, with varying TNP loadings (0, 0.25, 0.5, and 1%) examined for their impact on the film properties. DSC analysis showed that the glass transition temperature (T_g) of the NIPU films increased with TNP loading, due to enhanced crosslinking density and reduced chain mobility. Mechanical tests revealed a significant improvement in tensile strength from 0.33 MPa to 2.28 MPa with TNP addition, while elongation at break decreased, reflecting increased cross-linking. DMA results indicated a higher storage modulus (E') and $\tan\delta$, demonstrating enhanced stiffness and mechanical reinforcement. The water contact angle increased from 97° to 105° with TNP loading, indicating improved hydrophobicity due to the increased surface roughness. Antimicrobial tests showed that NT-*X* films effectively inhibited *Escherichia coli* and exhibited antifouling properties against *Staphylococcus aureus*. The antimicrobial activity is attributed to the photocatalytic properties of TNPs NPs, which generate reactive oxygen species (ROS) under light exposure. In summary, the TNP-incorporated NIPU films exhibited improved thermal stability, mechanical properties, hydrophobicity, and antimicrobial effectiveness compared to bare NIPU films, highlighting their potential for high-performance, environmentally friendly coating applications.

Data availability

All data are available in the manuscript and the data supporting this article have been included as part of the ESI.†

Author contributions

Jaydip D. Bhaliya: conceptualization, methodology, validation, investigation, data curation, and writing – original draft. S. N. Raju Kutcherlapati: supervision, resources, project administration, data curation, funding acquisition, review and editing, and visualization. Nikhil Dhore: synthesis part of CSBO, investigation, and data curation. Neelambaram Punugupati: investigation and data curation. Kavya Lekha Sunkara: antimicrobial studies and data validation. Sunil Misra: antimicrobial studies and data validation. Shivam Shailesh Kumar Joshi: investigation and data curation. All authors contributed to the final version of the manuscript. All authors approved the publication of this version of the manuscript. The authors declare no competing financial interest.

Conflicts of interest

There are no conflicts to declare.

Acknowledgements

K. S. N. R. and J. D. B. also acknowledge the Department of Science & Technology (DST) Science and Engineering Research Board (SERB) research grant (project no. SRG/2022/001789; project code: GAP 0949), DC&P, New Delhi (CoE-Polymer Coatings for Decorative, Protective & Strategic Applications) for financial support (25012/01/2020-PC-II) (FTS: 16020). K. S. N. R. and J. D. B. thank Dr P. Aruna for providing the CSBO for this research work. The authors also acknowledge CSIR-IICT, Hyderabad, for executing the research work (manuscript no. IICT/Pubs./2024/329). S. S. K. J. acknowledges the Department of Science & Technology (DST), New Delhi, India, for providing the INSPIRE fellowship (project no. DST/INSPIRE/IF220054). The authors also wish to acknowledge the help extended by Mrs Y. Swarna Latha, Mr L. Yugender Raju, Mr Arunava Dutta, and Mr Sandeep Kumar for their technical assistance provided during the investigation.

References

1 J. J. Bozell, Feedstocks for the future - Biorefinery production of chemicals from renewable carbon, *Clean: Soil, Air, Water*, 2008, **36**, 641–647, DOI: **10.1002/clen.200800100**.
2 M. A. R. Meier, Metathesis with Oleochemicals: New approaches for the utilization of plant oils as renewable resources in polymer science, *Macromol. Chem. Phys.*, 2009, **210**, 1073–1079, DOI: **10.1002/macp.200900168**.
3 Y. Xia, P. H. Henna and R. C. Larock, Novel thermosets from the cationic copolymerization of modified linseed oils and dicyclopentadiene, *Macromol. Mater. Eng.*, 2009, **294**, 590–598, DOI: **10.1002/mame.200900060**.

4 J. Thomas and M. D. Soucek, Cationic Copolymers of Norbornylized Seed Oils for Fiber-Reinforced Composite Applications, *ACS Omega*, 2022, **7**, 33949–33962, DOI: 10.1021/acsomega.2c02569.
5 Y. Xia and R. C. Larock, Castor oil-based thermosets with varied crosslink densities prepared by ring-opening metathesis polymerization (ROMP), *Polymer*, 2010, **51**, 2508–2514, DOI: 10.1016/j.polymer.2010.04.014.
6 J. Lu, S. Khot and R. P. Wool, New sheet molding compound resins from soybean oil. I. Synthesis and characterization, *Polymer*, 2005, **46**, 71–80, DOI: 10.1016/j.polymer.2004.10.060.
7 Z. Demchuk, O. Shevchuk, I. Tarnavchyk, V. Kirianchuk, A. Kohut, S. Voronov and A. Voronov, Free Radical Polymerization Behavior of the Vinyl Monomers from Plant Oil Triglycerides, *ACS Sustain. Chem. Eng.*, 2016, **4**, 6974–6980, DOI: 10.1021/acssuschemeng.6b01890.
8 V. Sharma and P. P. Kundu, Condensation polymers from natural oils, *Prog. Polym. Sci.*, 2008, **33**, 1199–1215, DOI: 10.1016/j.progpolymsci.2008.07.004.
9 Z. Wang, M. S. Ganewatta and C. Tang, Sustainable polymers from biomass: Bridging chemistry with materials and processing, *Prog. Polym. Sci.*, 2020, **101**, 101197, DOI: 10.1016/j.progpolymsci.2019.101197.
10 Y. Xia, Z. Zhang, M. R. Kessler, B. Brehm-Stecher and R. C. Larock, Antibacterial soybean-oil-based cationic polyurethane coatings prepared from different amino polyols, *ChemSusChem*, 2012, **5**, 2221–2227, DOI: 10.1002/cssc.201200352.
11 M. Burelo, A. Y. Yau, S. Gutiérrez, J. A. Cruz-Morales, G. Luna-Barcenas and C. D. Treviño-Quintanilla, Metathesis of butadiene rubber for the sustainable production of polyesters and polyols, *Polym. Degrad. Stab.*, 2024, **227**, 110874, DOI: 10.1016/j.polymdegradstab.2024.110874.
12 M. Burelo, A. Martínez, J. D. Hernández-Varela, T. Stringer, M. Ramírez-Melgarejo, A. Y. Yau, G. Luna-Bárcenas and C. D. Treviño-Quintanilla, Recent Developments in Synthesis, Properties, Applications and Recycling of Bio-Based Elastomers, *Molecules*, 2024, **29**, 387, DOI: 10.3390/molecules29020387.
13 A. Delavarde, G. Savin, P. Derkenne, M. Boursier, R. Morales-Cerrada, B. Nottelet, J. Pinaud and S. Caillol, Sustainable polyurethanes: toward new cutting-edge opportunities, *Prog. Polym. Sci.*, 2024, **151**, 101805, DOI: 10.1016/j.progpolymsci.2024.101805.
14 L. Poussard, J. Mariage, B. Grignard, C. Detrembleur, C. Jéroîme, C. Calberg, B. Heinrichs, J. De Winter, P. Gerbaux, J. M. Raquez, L. Bonnaud and P. Dubois, Non-Isocyanate Polyurethanes from Carbonated Soybean Oil Using Monomeric or Oligomeric Diamines to Achieve Thermosets or Thermoplastics, *Macromolecules*, 2016, **49**, 2162–2171, DOI: 10.1021/acs.macromol.5b02467.
15 A. Lee and Y. Deng, Green polyurethane from lignin and soybean oil through non-isocyanate reactions, *Eur. Polym. J.*, 2015, **63**, 67–73, DOI: 10.1016/j.eurpolymj.2014.11.023.
16 S. Gogoi and N. Karak, Biobased biodegradable waterborne hyperbranched polyurethane as an ecofriendly sustainable material, *ACS Sustain. Chem. Eng.*, 2014, **2**, 2730–2738, DOI: 10.1021/sc5006022.
17 L. Maisonneuve, O. Lamarzelle, E. Rix, E. Grau and H. Cramail, Isocyanate-Free Routes to Polyurethanes and Poly(hydroxy Urethane)s, *Chem. Rev.*, 2015, **115**, 12407–12439, DOI: 10.1021/acs.chemrev.5b00355.
18 A. A. Caraculacu and S. Coseri, Isocyanates in polyaddition processes. Structure and reaction mechanisms, *Prog. Polym. Sci.*, 2001, **26**, 799–851, DOI: 10.1016/S0079-6700(00)00033-2.
19 L. Hojabri, X. Kong and S. S. Narine, Fatty Acid-Derived diisocyanate and biobased polyurethane produced from vegetable oil: Synthesis, polymerization, and characterization, *Biomacromolecules*, 2009, **10**, 884–891, DOI: 10.1021/bm801411w.
20 L. Hojabri, X. Kong and S. S. Narine, Novel long chain unsaturated diisocyanate from fatty acid: Synthesis, characterization, and application in bio-based polyurethane, *J. Polym. Sci., Part A: Polym. Chem.*, 2010, **48**, 3302–3310, DOI: 10.1002/pola.24114.
21 A. S. More, D. V. Palaskar, E. Cloutet, B. Gadenne, C. Alfos and H. Cramail, Aliphatic polycarbonates and poly(ester carbonate)s from fatty acid derived monomers, *Polym. Chem.*, 2011, **2**, 2796–2803, DOI: 10.1039/C1PY00326G.
22 E. Hablot, B. Donnio, M. Bouquey and L. Avérous, Dimer acid-based thermoplastic bio-polyamides: Reaction kinetics, properties and structure, *Polymer*, 2010, **51**, 5895–5902, DOI: 10.1016/j.polymer.2010.10.026.
23 S. S. Kashyap, K. Borah, J. S. Shailesh Kumar, Z. Sheerazi, R. Narayan and M. Ahmed, Role of silicoaluminophosphate as a corrosion inhibiting nanocontainer and filler in environmentally benign bio-based hybrid coatings, *ACS Sustainable Resour. Manage.*, 2024, **1**, 1211–1224, DOI: 10.1021/acssusresmgt.4c00084.
24 L. Hojabri, X. Kong and S. S. Narine, Functional thermoplastics from linear diols and diisocyanates produced entirely from renewable lipid sources, *Biomacromolecules*, 2010, **11**, 911–918, DOI: 10.1021/bm901308c.
25 Z. S. Petrović, W. Zhang and I. Javni, Structure and properties of polyurethanes prepared from triglyceride polyols by ozonolysis, *Biomacromolecules*, 2005, **6**, 713–719, DOI: 10.1021/bm049451s.
26 A. Guo, D. Demydov, W. Zhang and Z. S. Petrovic, Polyols and polyurethanes from hydroformylation of soybean oil, *J. Polym. Environ.*, 2002, **10**, 49–52, DOI: 10.1023/A:1021022123733.
27 M. Desroches, S. Caillol, V. Lapinte, R. Auvergne and B. Boutevin, Synthesis of biobased polyols by thiol-ene coupling from vegetable oils, *Macromolecules*, 2011, **44**, 2489–2500, DOI: 10.1021/ma102884w.
28 C. Fu, Z. Zheng, Z. Yang, Y. Chen and L. Shen, A fully bio-based waterborne polyurethane dispersion from vegetable oils: From synthesis of precursors by thiol-ene reaction to

study of final material, *Prog. Org. Coat.*, 2014, **77**, 53–60, DOI: 10.1016/j.porgcoat.2013.08.002.

29 A. Adhvaryu and S. Z. Erhan, Epoxidized soybean oil as a potential source of high-temperature lubricants, *Ind. Crops Prod.*, 2002, **15**, 247–254, DOI: 10.1016/S0926-6690(01)00120-0.

30 Z. S. Petrović, A. Zlatanić, C. C. Lava and S. Sinadinović-Fišer, Epoxidation of soybean oil in toluene with peroxoacetic and peroxoformic acids - Kinetics and side reactions, *Eur. J. Lipid Sci. Technol.*, 2002, **104**, 293–299, DOI: 10.1002/1438-9312(200205)104:5<293::AID-EJLT293>3.0.CO;2-W.

31 A. S. More, L. Maisonneuve, T. Lebarbé, B. Gadenne, C. Alfos and H. Cramail, Vegetable-based building-blocks for the synthesis of thermoplastic renewable polyurethanes and polyesters, *Eur. J. Lipid Sci. Technol.*, 2013, **115**, 61–75, DOI: 10.1002/ejlt.201200172.

32 I. Javni, P. H. Doo and Z. S. Petrović, Soy-based polyurethanes by nonisocyanate route, *J. Appl. Polym. Sci.*, 2008, **108**, 3867–3875, DOI: 10.1002/app.27995.

33 N. Dhore, E. Prasad, R. Narayan, C. R. K. Rao and A. Palanisamy, Studies on Biobased Non-Isocyanate Polyurethane Coatings with Potential Corrosion Resistance, *Sustainable Chem.*, 2023, **4**, 95–109, DOI: 10.3390/suschem4010008.

34 M. Rayung, N. A. Ghani and N. Hasanudin, A review on vegetable oil-based non isocyanate polyurethane: towards a greener and sustainable production route, *RSC Adv.*, 2024, **14**, 9273–9299, DOI: 10.1039/d3ra08684d.

35 P. P. Pescarmona, Cyclic carbonates synthesised from CO_2: Applications, challenges and recent research trends, *Curr. Opin. Green Sustainable Chem.*, 2021, **29**, 100457, DOI: 10.1016/j.cogsc.2021.100457.

36 B. Wang, F. Wang, Y. Kong, Z. Wu, R. M. Wang, P. Song and Y. He, Polyurea-crosslinked cationic acrylate copolymer for antibacterial coating, *Colloids Surf., A*, 2018, **549**, 122–129, DOI: 10.1016/j.colsurfa.2018.04.012.

37 H. Gholami and H. Yeganeh, Soybean oil-derived non-isocyanate polyurethanes containing azetidinium groups as antibacterial wound dressing membranes, *Eur. Polym. J.*, 2021, **142**, 110142, DOI: 10.1016/j.eurpolymj.2020.110142.

38 H. Gholami and H. Yeganeh, Soybean Oil Derived Non-isocyanate Polyurethane with In Situ Formed Nano-silver as Antimicrobial Wound Dressing, in *Eco-friendly and Smart Polymer Systems*, ed. H. Mirzadeh, A. Katbab, ISPST 2018, Springer International Publishing, Cham, 2020, pp. 297–300, DOI: 10.1007/978-3-030-45085-4_71.

39 K. Borah, A. Palanisamy, R. Narayan, S. Satapathy, V. Dileepkumar and S. Misra, Structure-property relationship of thermoplastic polyurethane cationomers carrying quaternary ammonium groups, *React. Funct. Polym.*, 2022, **181**, 105447, DOI: 10.1016/j.reactfunctpolym.2022.105447.

40 E. A. Baroncini, S. Kumar Yadav, G. R. Palmese and J. F. Stanzione, Recent advances in bio-based epoxy resins and bio-based epoxy curing agents, *J. Appl. Polym. Sci.*, 2016, **133**, 44103, DOI: 10.1002/app.44103.

41 R. Chen, C. Zhang and M. R. Kessler, Polyols and polyurethanes prepared from epoxidized soybean oil ring-opened by polyhydroxy fatty acids with varying OH numbers, *J. Appl. Polym. Sci.*, 2015, **132**, 41213, DOI: 10.1002/app.41213.

42 E. Kinaci, E. Can, J. J. La Scala and G. R. Palmese, Influence of epoxidized cardanol functionality and reactivity on network formation and properties, *Polymers*, 2020, **12**, 1–14, DOI: 10.3390/polym12091956.

43 N. O. Shaker, E. M. Kandeel, E. E. Badr and M. M. El-Sawy, Synthesis and properties of renewable environment-friendly epoxy resins for surface coatings, *J. Dispersion Sci. Technol.*, 2008, **29**, 421–425, DOI: 10.1080/01932690701718800.

44 K. Błażek, P. Kasprzyk and J. Datta, Diamine derivatives of dimerized fatty acids and bio-based polyether polyol as sustainable platforms for the synthesis of non-isocyanate polyurethanes, *Polymer*, 2020, **205**, 122768, DOI: 10.1016/j.polymer.2020.122768.

45 J. Catalá, I. Guerra, J. M. García-Vargas, M. J. Ramos, M. T. García and J. F. Rodríguez, Tailor-Made Bio-Based Non-Isocyanate Polyurethanes (NIPUs), *Polymers*, 2023, **15**, 1589, DOI: 10.3390/polym15061589.

46 Y. Ecochard and S. Caillol, How to overcome limitations and reach cutting edge properties?, *Eur. Polym. J.*, 2020, **137**, 109915, DOI: 10.1016/j.eurpolymj.2020.109915.

47 P. Patel, F. M. de Souza and R. K. Gupta, Study of Soybean Oil-Based Non-Isocyanate Polyurethane Films via a Solvent and Catalyst-Free Approach, *ACS Omega*, 2024, **9**, 5862–5875, DOI: 10.1021/acsomega.3c09185.

48 V. Kostopoulos and E. Kollia, Development and Mechanical Characterization of a Non-Isocyanate Rigid Polyurethane Foam, *Res. Dev. Material. Sci.*, 2020, **10**, 1149–1156, DOI: 10.31031/rdms.2019.10.000738.

49 G. Kianpour, R. Bagheri, A. Pourjavadi and H. Ghanbari, In situ synthesized TiO_2-polyurethane nanocomposite for bypass graft application: In vitro endothelialization and degradation, *Mater. Sci. Eng., C*, 2020, **114**, 111043, DOI: 10.1016/j.msec.2020.111043.

50 S. I. Bhat and S. Ahmad, Castor oil-TiO_2 hyperbranched poly (ester amide) nanocomposite: a sustainable, green precursor-based anticorrosive nanocomposite coatings, *Prog. Org. Coat.*, 2018, **123**, 326–336, DOI: 10.1016/j.porgcoat.2018.06.010.

51 O. U. Rahman and S. Ahmad, Soy polyester urethane/TiO_2 and Ce-TiO_2 nanocomposites: Preparation, characterization and evaluation of electrochemical corrosion resistance performance, *RSC Adv.*, 2016, **6**, 10584–10596, DOI: 10.1039/c5ra23928a.

52 J. H. Xu, J. Y. Chen, Y. N. Zhang, T. Liu and J. J. Fu, A Fast Room-Temperature Self-Healing Glassy Polyurethane, *Angew. Chem., Int. Ed.*, 2021, **60**, 7947–7955, DOI: 10.1002/anie.202017303.

53 L. Meng, H. Qiu, D. Wang, B. Feng, M. Di, J. Shi and S. Wei, Castor-oil-based waterborne acrylate/SiO_2 hybrid coatings prepared via sol–gel and thiol-ene reactions, *Prog. Org.*

Coat., 2020, **140**, 105492, DOI: 10.1016/j.porgcoat.2019.105492.

54 C. Wang, F. Xu, M. He, L. Ding, S. Li and J. Wei, Castor oil-based polyurethane/silica nanocomposites: Morphology, thermal and mechanical properties, *Polym. Compos.*, 2018, **39**, E1800–E1806, DOI: 10.1002/pc.24798.

55 Z. Yu, Z. Wang, H. Li, J. Teng and L. Xu, Shape memory epoxy polymer (SMEP) composite mechanical properties enhanced by introducing graphene oxide (GO) into the matrix, *Materials*, 2019, **12**, 1107, DOI: 10.3390/ma12071107.

56 L. He, F. Xia, Y. Wang, J. Yuan, D. Chen and J. Zheng, Mechanical and dynamic mechanical properties of the amino silicone oil emulsion modified ramie fiber reinforced composites, *Polymers*, 2021, **13**, 4083, DOI: 10.3390/polym13234083.

57 H. Liang, L. Liu, J. Lu, M. Chen and C. Zhang, Castor oil-based cationic waterborne polyurethane dispersions: Storage stability, thermo-physical properties and antibacterial properties, *Ind. Crops Prod.*, 2018, **117**, 169–178, DOI: 10.1016/j.indcrop.2018.02.084.

58 Z. Yang, Y. Feng, H. Liang, Z. Yang, T. Yuan, Y. Luo, P. Li and C. Zhang, A Solvent-Free and Scalable Method to Prepare Soybean-Oil-Based Polyols by Thiol-Ene Photo-Click Reaction and Biobased Polyurethanes Therefrom, *ACS Sustain. Chem. Eng.*, 2017, **5**, 7365–7373, DOI: 10.1021/acssuschemeng.7b01672.

59 L. Nguyen Dang, S. Le Hoang, M. Malin, J. Weisser, T. Walter, M. Schnabelrauch and J. Seppälä, Synthesis and characterization of castor oil-segmented thermoplastic polyurethane with controlled mechanical properties, *Eur. Polym. J.*, 2016, **81**, 129–137, DOI: 10.1016/j.eurpolymj.2016.05.024.

60 M. Kathalewar, A. Sabnis and G. Waghoo, Effect of incorporation of surface treated zinc oxide on non-isocyanate polyurethane based nano-composite coatings, *Prog. Org. Coat.*, 2013, **76**, 1215–1229, DOI: 10.1016/j.porgcoat.2013.03.027.

61 K. M. Seeni Meera, R. Murali Sankar, J. Paul, S. N. Jaisankar and A. B. Mandal, The influence of applied silica nanoparticles on a bio-renewable castor oil based polyurethane nanocomposite and its physicochemical properties, *Phys. Chem. Chem. Phys.*, 2014, **16**, 9276–9288, DOI: 10.1039/c4cp00516c.

62 K. C. Chang, C. Y. Lin, H. F. Lin, S. C. Chiou, W. C. Huang, J. M. Yeh and J. C. Yang, Thermally and mechanically enhanced epoxy resin-silica hybrid materials containing primary amine-modified silica nanoparticles, *J. Appl. Polym. Sci.*, 2008, **108**, 1629–1635, DOI: 10.1002/app.27559.

63 Y. Xia and R. C. Larock, Preparation and properties of aqueous castor oil-based polyurethane-silica nanocomposite dispersions through a sol-gel process, *Macromol. Rapid Commun.*, 2011, **32**, 1331–1337, DOI: 10.1002/marc.201100203.

64 S. Doley and S. K. Dolui, Solvent and catalyst-free synthesis of sunflower oil based polyurethane through non-isocyanate route and its coatings properties, *Eur. Polym. J.*, 2018, **102**, 161–168, DOI: 10.1016/j.eurpolymj.2018.03.030.

65 H. Peng, Z. Zhang and Z. Wang, Dispersion of TiO_2 nanoparticles in TiO_2/HIPS composites, *J. Dispersion Sci. Technol.*, 2005, **26**, 203–206, DOI: 10.1081/DIS-200045593.

66 J. Zhou, B. Hao, L. Wang, J. Ma and W. Cheng, Preparation and characterization of nano-TiO_2/chitosan/poly(N-isopropylacrylamide) composite hydrogel and its application for removal of ionic dyes, *Sep. Purif. Technol.*, 2017, **176**, 193–199, DOI: 10.1016/j.seppur.2016.11.069.

67 Y. Liu, D. Sun, S. Askari, J. Patel, M. Macias-Montero, S. Mitra, R. Zhang, W. F. Lin, D. Mariotti and P. Maguire, Enhanced Dispersion of TiO_2 Nanoparticles in a TiO_2/PEDOT:PSS Hybrid Nanocomposite via Plasma-Liquid Interactions, *Sci. Rep.*, 2015, **5**, 15765, DOI: 10.1038/srep15765.

68 M. J. Nine, M. A. Cole, L. Johnson, D. N. H. Tran and D. Losic, Robust Superhydrophobic Graphene-Based Composite Coatings with Self-Cleaning and Corrosion Barrier Properties, *ACS Appl. Mater. Interfaces*, 2015, **7**, 28482–28493, DOI: 10.1021/acsami.5b09611.

69 E. Arezoo, E. Mohammadreza, M. Maryam and M. N. Abdorreza, The synergistic effects of cinnamon essential oil and nano TiO_2 on antimicrobial and functional properties of sago starch films, *Int. J. Biol. Macromol.*, 2020, **157**, 743–751, DOI: 10.1016/j.ijbiomac.2019.11.244.

70 M. R. Shaik, M. Alam and N. M. Alandis, Development of castor oil based poly(urethane-esteramide)/TiO_2 nanocomposites as anticorrosive and antimicrobial coatings, *J. Nanomater.*, 2015, **2015**, 1–10, DOI: 10.1155/2015/745217.

71 M. Hermansson, The DLVO theory in microbial adhesion, *Colloids Surf., B*, 1999, **14**, 105–119, DOI: 10.1016/S0927-7765(99)00029-6.

72 T. R. Garrett, M. Bhakoo and Z. Zhang, Bacterial adhesion and biofilms on surfaces, *Prog. Nat. Sci.*, 2008, **18**, 1049–1056, DOI: 10.1016/j.pnsc.2008.04.001.